

JET NOISE MODELLING USING AN ACOUSTIC ANALOGY

**Mohammed Z. Afsar, Sergey A. Karabasov, Tom P. Hynes, Ann P. Dowling and
Elena de la Rosa Blanco**

*Department of Engineering University of Cambridge
1, JJ Thompson Avenue, Cambridge CB3 0D
Email: ma357@cam.ac.uk*

Key words: jet noise, acoustic analogy, turbulence modelling

Abstract. Many jet noise prediction schemes are based on the acoustic analogy. The analogy allows one to calculate the overall sound pressure level at a point far away from the jet flow, and gives the solution as a volume integral over the region of turbulence. The terms under this integral sign involve a product of a wave propagation tensor and, a turbulent field tensor, that represents the fluctuating motions of the jet.

In this paper we examine the turbulent field tensor, and develop a model that captures its principal components. The model approximates the formal condition of statistical anisotropy. We analyse a high Reynolds number subsonic jet flow, and show the jet noise predictions using our model compares very well against experiment. The mean flow is obtained from a Reynolds Averaged Navier Stokes (RANS) calculation, and the turbulence statistics are found by calculating required properties using a Large Eddy Simulation (LES).

1. INTRODUCTION

Jet noise generation models are often formulated using an acoustic analogy¹. The analogy enables one to quantify overall sound pressure far away from the region of turbulent activity. It involves re-arranging the Navier-Stokes equations so that the linear fluctuations (from any base flow) appear on the left hand side, and the non-linear fluctuations are put to the right hand side. The linear fluctuations represent the acoustic propagation and the non-linear terms are the sources of the noise. The far field power spectral density of the fluctuating pressure can then be written as a volume integral over the region of turbulence. The integrand of the power spectrum is a product of two terms: the wave propagation tensor and the turbulent field tensor. In this paper we concentrate on the turbulent field tensor, and, in particular, on its kinematic representation.

The real difficulty in developing a mathematical model of jet noise is what form the turbulent field tensor should take. Mathematically, it is defined as cross power spectral density of the fluctuating Reynolds stress source term in the momentum equation. And since it involves the two-point, two-time, correlation of a velocity product, it is a tensor of 4th rank. Now, the simplest approach one can take is to assume the field is kinematically isotropic. In this case, the 4th rank tensor reduces to a single component. The assumption of isotropy, however, is naturally restrictive because it implies the absence of any preferred direction; that is certainly not the case for a jet

flow—the mean flow naturally imposes a preferred direction. A more realistic approach therefore is to model the tensor by supposing it to be *anisotropic*.

The effect of anisotropy has been the subject of much concern in jet noise. For example, Townsend showed a marked reduction in the integral length scale of the turbulence could certainly occur because of the lateral compression in the eddy structure. As a typical “eddy” cascades through the inertial subrange of a turbulent shear flow, it cannot remain isotropic. The large scales eddies are stretched and attain a thin cylindrical-like structure. Studies into the effect of anisotropy on jet noise began with Kraichnan’s work². He introduced a scale parameter to represent the elongation of the eddy structure in the direction of mean flow. Kraichnan’s results showed, the far field pressure spectrum could be very sensitive to this scale parameter. Goldstein and Rosenbaum³ also analyzed this problem; but their aim was to develop a noise generation model. They showed, it was the high frequency components of the source that were beamed downstream as parameter representing the anisotropy was varied.

Our aim in this paper is to provide a simple anisotropic representation of the turbulent field tensor. The symmetry between the tensor indices implies the fourth rank tensor, itself, will only possess 36 independent components. We show a formal anisotropic representation of the turbulent field tensor can capture its principal components. However, such a representation will be sensitive to the numerical resolution of those particular components. We, therefore, develop a simple approximation to the condition of anisotropy, that is designed to avoid the components that are difficult to capture numerically. Our results show jet noise predictions based on the *anisotropic approximation* are in reasonable agreement with experiment; both for the peak noise and the large angle spectra, at 90° .

We restrict the analysis to a cold jet flow and compare our results to the condition of isotropy. The acoustic analogy we use, is based on Goldstein’s linearized Euler equation system⁴; and we solve the wave propagation problem for a parallel shear layer defined locally, as a piece-wise constant approximation to the evolving mean flow; that is, by ignoring the gradients in the x-direction. We obtain the mean flow from a Reynolds Averaged Navier Stokes (RANS) calculation of a round jet: Reynolds number of 10^6 , and Mach number at nozzle exit of 0.75. The source statistics are found by calculating required turbulence properties using a Large Eddy Simulation (LES). We focus on noise predictions at an observation angles of 90° and 30° to the jet axis. For both of these cases, we compare our predictions to experiment results⁵.

2. ACOUSTIC ANALOGY

2.1. Governing Equations

Imagine a region of turbulence convected by a jet flow. The turbulent field is confined to a region near the jet, so that at large distances from the flow, all of the turbulent motion has ceased. Within the jet region, momentum is transferred in a random fashion, the jet flow interacts with this transfer causing energy changes in the field. The physical processes of *momentum transfer* and *energy change* are governed by the Navier Stokes equations, and generate acoustic waves that propagate to the far field.

The outcome of this section is Eq. (25)—a formula for the power spectral density of the far field pressure due to the turbulent activity in the jet flow. We represent the turbulent field by a ‘source term,’ which is simply a stationary random function described by field variables (y, τ) . The sources represent the dynamics of the turbulent

field and generate noise in the far field, at the observer position (x, t) . A picture of the jet flow is shown in Fig. (1).

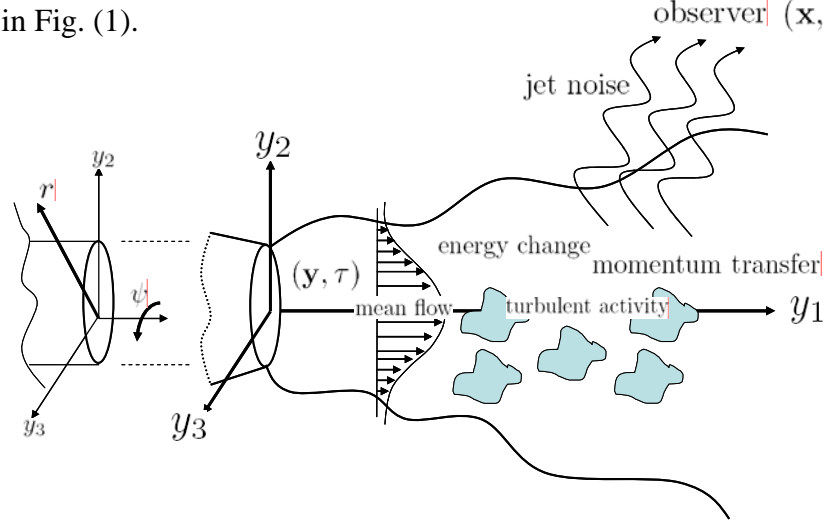


Figure 1: Coordinate system for a jet flow

We define the analogy using the linearized Euler equations formulated by Goldstein. In his system, the Euler equations are linearized about a base flow with density $\bar{\rho}$, pressure \bar{p} , and velocity \tilde{v}_j . The bar and single prime represent the time average and its perturbation, and the tilde and double prime represent the Favre average and its perturbation. The averaging operations are defined in the usual way:

$$\overline{(\bullet)}(y) \equiv \lim_{T \rightarrow \infty} \frac{1}{2T} \int_{-T}^T (\bullet)(y, \tau) d\tau \quad \text{and} \quad \bar{\rho}(\tilde{\bullet}) \equiv \overline{\rho(\bullet)}. \quad (1)$$

The momentum variable is defined with zero time average, $u_i = \rho v_i''$; and the Favre averaged stagnation enthalpy, and its perturbation, take the special definitions:

$$\tilde{h}_o = \tilde{h} + \frac{1}{2} \tilde{v}^2 \quad \text{and} \quad h_o'' = h'' + \tilde{v}_i v_i'' + \frac{1}{2} v''^2. \quad (2)$$

The system is given by the set of equations:

$$\frac{\partial \rho'}{\partial \tau} + \frac{\partial}{\partial y_j} (\rho' \tilde{v}_j + u_j) = 0 \quad (3)$$

$$\frac{\partial u_i}{\partial \tau} + \frac{\partial}{\partial y_j} (\tilde{v}_j u_i) + \frac{\partial p'}{\partial y_i} + u_j \frac{\partial \tilde{v}_i}{\partial y_j} - \left(\frac{\rho'}{\bar{\rho}} \right) \frac{\partial \tilde{\tau}_{ij}}{\partial y_j} = \frac{\partial T'_{ij}}{\partial y_j} \quad i = 1, \dots, 3. \quad (4)$$

$$\left(\frac{1}{\gamma - 1} \right) \frac{\partial p'}{\partial \tau} + \left(\frac{1}{\gamma - 1} \right) \frac{\partial}{\partial y_j} (p' \tilde{v}_j) + \frac{\partial}{\partial y_j} (u_j \tilde{h}) + p' \frac{\partial \tilde{v}_j}{\partial y_j} - \left(\frac{u_i}{\bar{\rho}} \right) \frac{\partial \tilde{\tau}_{ij}}{\partial y_j} = Q. \quad (5)$$

(Throughout this paper, summation applies across repeated indices.)

(The specific heat capacities of air, $\gamma = 1.4$.)

The nice feature of Goldstein's equations are the source terms, which are in a simple form, viz.:

$$\underbrace{T'_{ij} = -(\rho v_i'' v_j'' - \bar{\rho} \widetilde{v_i'' v_j''})}_{\text{Noise due to momentum transfer}} \quad (6)$$

$$Q = \underbrace{-\tilde{v}_j \frac{\partial T'_{ij}}{\partial y_i} + \frac{1}{2} \delta_{ij} \left[\frac{DT'_{ij}}{D\tau} + \frac{\partial \tilde{v}_k}{\partial y_k} T'_{ij} \right]}_{\text{Noise due to energy change}} - \underbrace{\frac{\partial}{\partial y_j} (\rho v_j'' h_o'' - \bar{\rho} \widetilde{v_j'' h_o''})}_{\text{Noise due to enthalpic heating}}. \quad (7)$$

In this paper, however, we concentrate on the cold jet flow where the noise from enthalpic heating is negligible compared to momentum transfer. Moreover, for the same reason, the perturbations in density can be neglected, i.e. $\rho(y, \tau) \approx \bar{\rho}(y)$. Then, the source terms reduce to:

$$T'_{ij} = -\bar{\rho} (v_i'' v_j'' - \widetilde{v_i'' v_j''}) \quad (8)$$

$$Q = -\tilde{v}_j \frac{\partial T'_{ij}}{\partial y_i} + \frac{1}{2} \delta_{ij} \left[\frac{DT'_{ij}}{D\tau} + \frac{\partial \tilde{v}_k}{\partial y_k} T'_{ij} \right]. \quad (9)$$

$D/D\tau$ is the usual convective derivative, given by:

$$\frac{D}{D\tau} = \frac{\partial}{\partial \tau} + \tilde{v}_j \frac{\partial}{\partial y_j}. \quad (10)$$

The tensor, $\tilde{\tau}_{ij}$, defined by $\tilde{\tau}_{ij} = \delta_{ij} \bar{p} + \bar{\rho} \widetilde{v_i'' v_j''}$, appears in the propagation operator of the linearized equations. It drives the jet evolution in the flow by interacting with the mean pressure. For a parallel mean flow the vector $\partial \tilde{\tau}_{ij} / \partial y_i$ is identically zero.

2.2. Representation Theorem

The wave propagation problem is solved in the frequency domain using the adjoint Green function. This method has been used many times in the past, for example the work by Dowling et al⁶, and by Tam and Auriant⁷. The adjoint Green function method is advantageous because it allows one to specify the turbulent field for a particular observer point. The method amounts to solving a set of homogeneous differential equations (when the right hand side is zero) in the jet region. Any unknown constants are easily found, because this solution in the jet must reduce to the solution of the wave equation in the far field, where the mean flow is all zero. In this paper we use the Fourier transform pair (with angular frequency ω):

$$\hat{f}(\omega) = \int_{-\infty}^{\infty} f(\tau) e^{-i\omega\tau} d\tau \quad \text{and} \quad f(\tau) = \frac{1}{2\pi} \int_{-\infty}^{\infty} \hat{f}(\omega) e^{i\omega\tau} d\omega. \quad (11)$$

It is algebraically straightforward to formulate a representation theorem for the far field pressure. For example, by taking the momentum-like adjoint Green function and performing the inner product of this, and the momentum equation (Eq. 4), gives the *adjoint momentum equation*. One must integrate each term by parts and apply the divergence theorem; we have to suppose, then, that any surface terms at infinity, far

away from the jet, are zero. A similar operation gives the *adjoint mass equation* and *adjoint energy equation*. Hence, the representation theorem for the far field pressure is:

$$\hat{p}(x, \omega) = - \int_{v_\infty(y)} \left(\hat{G}_i(y, \omega | x) \frac{\partial \hat{T}_{ij}}{\partial y_j}(y, \omega) + \hat{G}_4(y, \omega | x) \hat{Q}(y, \omega) \right) d^3 y. \quad (12)$$

$\hat{T}_{ij}(y, \omega)$ is the Fourier transform of $T'_{ij}(y, \tau)$, and $\hat{G}(y, \omega | x)$, the Fourier transform of the adjoint Green's function, satisfies the *adjoint equations*:

$$i\omega \hat{G}_o + \tilde{v}_j \frac{\partial \hat{G}_o}{\partial y_j} + \left(\frac{\hat{G}_i}{\bar{\rho}} \right) \frac{\partial \tilde{\tau}_{ij}}{\partial y_j} = 0 \quad (13)$$

$$i\omega \hat{G}_j + \frac{\partial \hat{G}_o}{\partial y_j} + \tilde{v}_i \frac{\partial \hat{G}_j}{\partial y_i} - \hat{G}_i \frac{\partial \tilde{v}_i}{\partial y_j} + \tilde{h} \frac{\partial \hat{G}_4}{\partial y_j} + \left(\frac{\hat{G}_4}{\bar{\rho}} \right) \frac{\partial \tilde{\tau}_{ij}}{\partial y_i} = 0 \quad j = 1, \dots, 3. \quad (14)$$

$$\left(\frac{i\omega}{\gamma - 1} \right) \hat{G}_4 + \left(\frac{\tilde{v}_j}{\gamma - 1} \right) \frac{\partial \hat{G}_4}{\partial y_j} - \hat{G}_4 \frac{\partial \tilde{v}_j}{\partial y_j} + \frac{\partial \hat{G}_j}{\partial y_j} = \delta(y - x). \quad (15)$$

\hat{G}_o is the adjoint density-like variable and $\hat{G}_1 - \hat{G}_3$ are the adjoint momentum-like variables. \hat{G}_4 , the pressure-like quantity, is the variable in the adjoint energy equation.

2.3. An equivalent representation theorem: far field pressure budget

An important aspect of the present analysis is that the source term in the representation theorem is \hat{T}_{ij} only. The term Q , is, a function of \hat{T}_{ij} as well---see Eq. (9). If we now insist that \hat{T}_{ij} is *continuous* throughout the field space (y, τ) we can integrate Eq. (12) by parts. It seems sensible to do this. Computing spatial derivatives of a function that we can, at best, model, would be numerically challenging. Especially given that one would be relying upon a CFD solution that is only ever known on a discrete set of points. The Green function, on the other hand, can be determined, and differentiated, with accuracy. Substituting Eq. (9) into Eq. (12) and integrating each term by parts, so that we isolate \hat{T}_{ij} , gives the equivalent sound field representation:

$$\hat{p}(x, \omega) = \int_{v_\infty(y)} \hat{I}_{ij}(y, \omega | x) \hat{T}_{ij}(y, \omega) d^3 y. \quad (16)$$

\hat{I}_{ij} is a propagation tensor defined by:

$$\begin{aligned} \hat{I}_{ij}(y, \omega | x) = & \frac{\partial \hat{G}_j}{\partial y_i}(y, \omega | x) - \left[\frac{\partial \tilde{v}_j}{\partial y_i}(y) \hat{G}_4(y, \omega | x) + \tilde{v}_j(y) \frac{\partial \hat{G}_4}{\partial y_i}(y, \omega | x) \right] \\ + & \frac{\delta_{ij}}{2} \left[i\omega \left(1 + \frac{\tilde{v}_k}{i\omega} \frac{\partial}{\partial y_k} \right) \hat{G}_4(y, \omega | x) - \frac{\partial \tilde{v}_k}{\partial y_k}(y) \hat{G}_4(y, \omega | x) \right]. \end{aligned} \quad (17)$$

The equivalent representation states, mathematically, what we said in words at the beginning of this section. For a cold jet flow, momentum transfer and energy change in the field of turbulence (through \hat{T}_{ij}) generates acoustic waves (through Green function terms) that propagate to the far field.

2.4. Power spectral density formula

The power spectral density of the far field pressure is:

$$\hat{P}(x, \omega) = \int_{v_\infty(y)} \int_{v_\infty(\eta)} \hat{I}_{ijkl}(y, \eta, \omega | x) \hat{R}_{ij,kl}(y, \eta, \omega) d^3\eta d^3y. \quad (18)$$

η is the vector separation between the correlation positions y and $y + \eta$; in Cartesian coordinates $\eta = (\eta_1, \eta_2, \eta_3)$. The integrand is expressed in terms of the 4th rank tensors: $\hat{I}_{ijkl}(y, \eta, \omega | x)$ ---for the wave propagation, and $\hat{R}_{ijkl}(y, \eta, \omega)$ for the turbulent field. They are easily defined from standard theory⁸, i.e.,

$$\hat{I}_{ijkl}(y, \eta, \omega | x) = \hat{I}_{ij}(y, -\omega | x) \hat{I}_{kl}(y + \eta, \omega | x), \quad (19)$$

where the second rank tensors \hat{I}_{ij} are given by Eq. (17). $\hat{R}_{ijkl}(y, \eta, \omega)$, the 4th rank cross power spectral density of the stationary random function \hat{T}_{ij} is:

$$\begin{aligned} \hat{R}_{ij,kl}(y, \eta, \omega) &= \int_{-\infty}^{+\infty} R_{ij,kl}(y, \eta, \tau_0) e^{-i\omega\tau_0} d\tau_0 \\ &= \int_{-\infty}^{+\infty} \overline{T'_{ij}(y, \tau) T'_{kl}(y + \eta, \tau + \tau_0)} e^{-i\omega\tau_0} d\tau_0. \end{aligned} \quad (20)$$

We simplify the wave propagation tensor \hat{I}_{ijkl} by assuming the variation of second rank tensor \hat{I}_{kl} is small over η_2 and η_3 compared to the correlation length. The dependence on η_1 can be approximated, for example, by following Tam and Auriant⁹, i.e.,

$$\hat{I}_{kl}(y + \eta, \omega | x) \approx \hat{I}_{kl}(y, \omega | x) e^{ik_o \eta_1 \cos\theta} \quad (21)$$

where the observer is in the far field at an angle θ to the jet flow; and $k_o = \omega / c_\infty$ is the wave number in the far field. The power spectral density then simplifies to,

$$\hat{P}(x, \omega) = \int_{v_\infty(y)} \hat{I}_{ij}(y, -\omega | x) \hat{I}_{kl}(y, \omega | x) \int_{v_\infty(\eta)} \hat{R}_{ij,kl}(y, \eta, \omega) e^{ik_o \eta_1 \cos \theta} d^3 \eta d^3 y \quad (22)$$

We will find it useful to label $\hat{I}_{ijkl}(y, \omega | x)$ as

$$\hat{I}_{ijkl}(y, \omega | x) = \hat{I}_{ij}(y, -\omega | x) \hat{I}_{kl}(y, \omega | x); \quad (23)$$

and the integral of the turbulent field tensor over η , $\hat{R}_{ij,kl}^{\text{total}}(y, \omega)$, as

$$\hat{R}_{ij,kl}^{\text{total}}(y, \omega) = \int_{v_\infty(\eta)} \hat{R}_{ij,kl}(y, \eta, \omega) e^{ik_o \eta_1 \cos \theta} d^3 \eta. \quad (24)$$

Then, the final form of power spectral density is rather easier to handle.

$$\hat{P}(x, \omega) = \int_{v_\infty(y)} \hat{I}_{ijkl}(y, \omega | x) \hat{R}_{ij,kl}^{\text{total}}(y, \omega) d^3 y \quad (25)$$

The rest of this paper is devoted to analyzing Eq. (25) for a parallel shear flow. We adopt a cylindrically based coordinate system for a jet flow that is circular cylindrical, so that the field spaces are $y = (y_1, r, \psi)$ and $x = (x_1, R, \Psi)$. The mean flow is directed axially in y_1 , and a function of r ; and the observer is in the far field at an angle θ to the jet axis. To evaluate the wave propagation tensor, \hat{I}_{ijkl} (using Eqs. 17 & 23), we require a Green function solution for a locally parallel flow. That problem is relatively straightforward; for example, the method used by Afsar et al¹⁰ is quite convenient for a CFD based mean flow. For the turbulent field tensor $\hat{R}_{ij,kl}$, on other hand, we must resort to simple modeling. We proceed along a hierarchy of increasing complexity. In section 3 we suppose the statistical function $R_{ij,kl}(y, \eta, \tau_0)$ is isotropic in its tensor indices, then, in section 4 we present a complete anisotropic representation of the tensor. Finally, in section 5, we approximate the formula for statistical anisotropy to avoid the components that are difficult to resolve numerically. In all cases, we compare our predictions with the noise data from experiment.

3. STATISTICAL ISOTROPY: MODEL $R_{ij,kl}(y, \eta, \tau_0)$

3.1. Definition

If we suppose the statistical function $R_{ij,kl}(y, \eta, \tau_0)$ is isotropic and symmetric in all its tensor indices, then:

$$R_{ij,kl}(y, \eta, \tau_0) = (\delta_{ij} \delta_{kl} + \delta_{ik} \delta_{jl} + \delta_{il} \delta_{jk}) F(y, \eta, \tau_0) \quad (26)$$

The scalar function, $F(y, \eta, \tau_0) = \frac{1}{3} R_{11,11}(y, \eta, \tau_0)$. Under statistical isotropy the Fourier transform of $R_{ij,kl}(y, \eta, \tau_0)$ is:

$$\hat{R}_{ij,kl}(y, \eta, \omega) = \left(\delta_{ij} \delta_{kl} + \delta_{ik} \delta_{jl} + \delta_{il} \delta_{jk} \right) \frac{1}{3} \int_{-\infty}^{+\infty} R_{11,11}(y, \eta, \tau_0) e^{-i\omega\tau_0} d\tau_0. \quad (27)$$

3.2. Power spectral density

Substituting Eq. (27) into the power spectral density formula Eq. (25) gives,

$$\hat{P}(x, \omega) = \frac{1}{3} \int_{V_\infty(y)} \left(\hat{I}_{jjkk}(y, \omega | x) + \hat{I}_{jkjk}(y, \omega | x) + \hat{I}_{jkkj}(y, \omega | x) \right) \hat{R}_{11,11}^{\text{total}}(y, \omega) d^3 y \quad (28)$$

The quadratic forms, $(\hat{I}_{jjkk}, \hat{I}_{jkjk}, \hat{I}_{jkkj})$, can easily be found using Eqs. (17) and (23). We note here the biggest contribution to the power spectrum will come from the Hermitian quadratic form \hat{I}_{jkjk} .

3.3. $R_{11,11}(y, \eta, \tau_0)$

In this paper we use a Gaussian model for $R_{11,11}(y, \eta, \tau_0)$, suggested by Tam and Auriant¹⁰,

$$R_{11,11}(y, \eta, \tau_0) = A^2(y) \exp \left(-\frac{|\eta_1|}{U(y)\tau_s} - \frac{\ln 2}{l_s^2} \left[(\eta_1 - U(y)\tau_s)^2 + \eta_2^2 + \eta_3^2 \right] \right) \quad (29)$$

The Gaussian model is defined by three quantities: a characteristic length scale, l_s ; time scale, τ_s ; and the amplitude of $R_{11,11}(y, \eta, \tau_0)$, A . We suppose this amplitude function is proportional to the turbulent kinetic energy. Indeed the constant of proportionality can easily be found by comparing the amplitude to the turbulent kinetic energy from the RANS calculation. The comparison is made at several locations along the shear layer, near to the nozzle, and far downstream towards the end of the potential core. We have found this constant of proportionality does not vary significantly and the subsequent calculations are therefore made using its value at the end of the potential core.

The characteristic scales are found numerically, by comparing Eq. (29) with the correlation function $R_{11,11}(y, \eta, \tau_0)$ calculated using a Large Eddy Simulation¹¹. In Fig. 2 we show this Gaussian fit is a reasonable representation of the correlation function at a typical location, near the end of the potential core of the jet, along the shear layer, $r = 0.5 D_{\text{jet}}$.

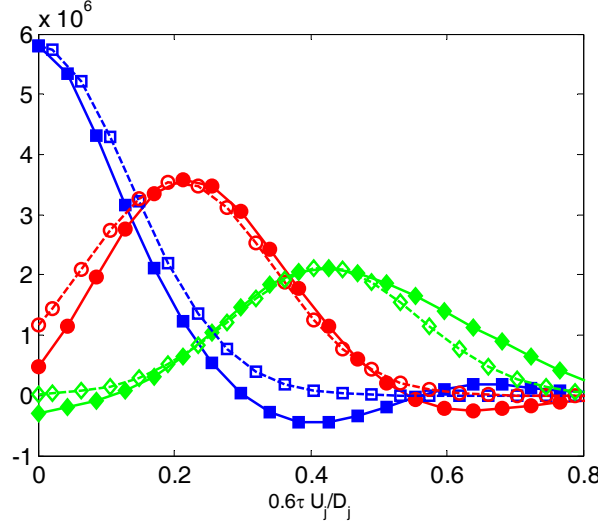


Figure 2: $R_{11,11}(y, \eta, \tau_0)$, location: $y_1/D_{\text{jet}} = 4$ and $r/D_{\text{jet}} = 0.5$; Gaussian fit = open symbol and dashed line, LES data = filled symbol and solid line.

To use the Gaussian model in our power spectral density formula, however, we have to first take the Fourier transform, and then integrate in η . Those steps are quite straightforward, and have been spelled out before, we just the final result:

$$\begin{aligned} \hat{R}_{11,11}^{\text{total}}(y, \omega) &= \int_{v_\infty(\eta)} \hat{R}_{11,11}(y, \eta, \omega) e^{ik_o \eta_1 \cos \theta} d^3 \eta \\ &= 2A^2(y) \left(\frac{\pi}{\ln 2} \right)^{\frac{3}{2}} l_s^3 \tau_s \exp \left(-\frac{\omega^2 l_s^2}{4U^2(y) \ln 2} \right) \frac{1}{1 + \omega^2 \tau_s^2 \left(1 - \frac{U(y)}{c_\infty} \cos \theta \right)^2}. \end{aligned} \quad (30)$$

3.4. Predicted noise spectra

We present sound predictions for a round jet with Reynolds number of 10^6 and the Mach number of 0.75. Throughout this paper the Green function is defined locally, at every axial mean flow location, based on the RANS data. In Fig. (3a) we show the predicted noise spectrum at 90° , and in Fig. (3b) we show peak jet noise spectrum at 30° to the jet axis. Notice the under statistical isotropy the peak noise, at 30° to the jet axis, is predicted very well. However, for the 90° spectrum, the peak noise is overpredicted by 8 dB. For both of these calculations, we emphasise there are no empirical constants— $R_{11,11}$ is determined by direct comparison with the near-field LES data.

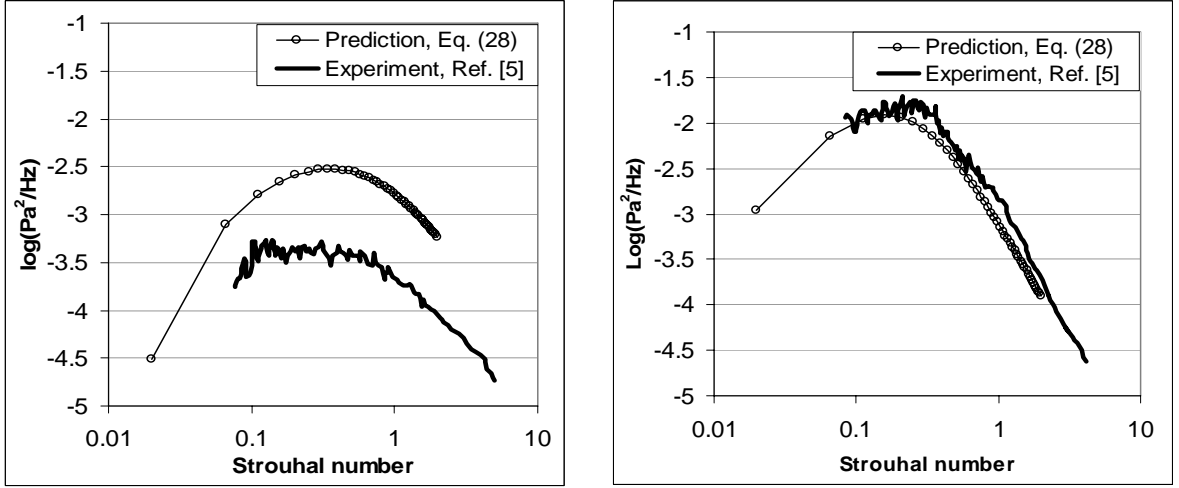


Figure 3: Condition of Statistical Isotropy: comparison of predictions made using Eq. (28) and Experiment⁵. Strouhal Number = $\omega D_{jet} / 2\pi U_{jet}$ (ω is the angular frequency rad/s; D_{jet} is the nozzle exit diameter, and U_{jet} is the nozzle exit velocity).

4. STATISTICAL ANISOTROPY: MODEL $R_{ij,kl}(y, \eta, \tau_0)$ SUPPOSING AXIAL SYMMETRY

In reality, the turbulent field tensor $R_{ij,kl}$ possesses 36 independent components. One can certainly include all 36 of these terms into the expression for $R_{ij,kl}$; however, for an axi-symmetric jet flow, most of them will be small in comparison to the longitudinal component $R_{11,11}$. As we saw earlier, under the conditions of isotropy---whether instantaneous or statistical---one component of the fourth rank tensor is retained, which we took to be $R_{11,11}$. Turbulent shear flows will be subject to anisotropic effects to a certain degree. It makes sense, then, to approximate $R_{ij,kl}$ to account for the general dynamics of the turbulent field, principally: the longitudinal term, $R_{11,11}$ (*stretching behavior*); the lateral term, $R_{22,22}$ (*compressing behavior*); and the deviatoric terms, $R_{12,12}$ & $R_{23,23}$ (*shearing behavior*).

4.1. Definition

If $R_{ij,kl}(y, \eta, \tau_0)$ has symmetry about the axial direction, then we can express it in terms of a number of scalar functions, i.e.

$$\begin{aligned}
R_{ij,kl}(y, \eta, \tau_0) = & \delta_{ij}\delta_{kl}\alpha_1(y, \eta, \tau_0) + \delta_{ik}\delta_{jl}\alpha_2(y, \eta, \tau_0) + \delta_{il}\delta_{jk}\alpha_3(y, \eta, \tau_0) \\
& + \delta_{ij}\delta_{k1}\delta_{l1}\alpha_4(y, \eta, \tau_0) + \delta_{kl}\delta_{i1}\delta_{j1}\alpha_5(y, \eta, \tau_0) + \delta_{jl}\delta_{i1}\delta_{k1}\alpha_6(y, \eta, \tau_0) \\
& + \delta_{ik}\delta_{j1}\delta_{l1}\alpha_7(y, \eta, \tau_0) + \delta_{jk}\delta_{i1}\delta_{l1}\alpha_8(y, \eta, \tau_0) + \delta_{il}\delta_{j1}\delta_{k1}\alpha_9(y, \eta, \tau_0) \\
& + \delta_{i1}\delta_{j1}\delta_{k1}\delta_{l1}\alpha_{10}(y, \eta, \tau_0)
\end{aligned} \tag{31}$$

Symmetry implies, $R_{ij,kl} = R_{ji,kl}$ and $R_{ij,kl} = R_{ij,lk}$. Then the number of scalar functions reduces, viz.

$$\begin{aligned}
R_{ij,kl}(y, \eta, \tau_0) = & \delta_{ij}\delta_{kl}\alpha_1(y, \eta, \tau_0) + [\delta_{ik}\delta_{jl} + \delta_{il}\delta_{jk}] \alpha_2(y, \eta, \tau_0) \\
& + \delta_{kl}\delta_{il}\delta_{j1}\alpha_4(y, \eta, \tau_0) + \delta_{ij}\delta_{k1}\delta_{l1}\alpha_5(y, \eta, \tau_0) \\
& + [\delta_{jl}\delta_{i1}\delta_{k1} + \delta_{ik}\delta_{j1}\delta_{l1} + \delta_{jk}\delta_{i1}\delta_{l1} + \delta_{il}\delta_{j1}\delta_{k1}] \alpha_6(y, \eta, \tau_0) \\
& + \delta_{i1}\delta_{j1}\delta_{k1}\delta_{l1}\alpha_{10}(y, \eta, \tau_0)
\end{aligned} \tag{32}$$

In this equation, the scalar functions are found by substituting a set of integer values for the tensor indices. For example, if we set $(i, j, k, l) = (1, 1, 1, 1)$; $(i, j, k, l) = (2, 2, 2, 2)$; $(i, j, k, l) = (1, 2, 1, 2)$; $(i, j, k, l) = (2, 3, 2, 3)$; $(i, j, k, l) = (1, 1, 2, 2)$, or $(i, j, k, l) = (2, 2, 1, 1)$ etc., we get six independent equations. The scalar functions then follow quite easily by solving those equations, viz.,

$$\begin{aligned}
\alpha_1(y, \eta, \tau_0) & = R_{22,22}(y, \eta, \tau_0) - 2R_{23,23}(y, \eta, \tau_0) \\
\alpha_2(y, \eta, \tau_0) & = R_{23,23}(y, \eta, \tau_0) \\
\alpha_4(y, \eta, \tau_0) & = R_{11,22}(y, \eta, \tau_0) - R_{22,22}(y, \eta, \tau_0) + 2R_{23,23}(y, \eta, \tau_0) \\
\alpha_5(y, \eta, \tau_0) & = R_{22,11}(y, \eta, \tau_0) - R_{22,22}(y, \eta, \tau_0) + 2R_{23,23}(y, \eta, \tau_0) \\
\alpha_6(y, \eta, \tau_0) & = R_{12,12}(y, \eta, \tau_0) - R_{23,23}(y, \eta, \tau_0) \\
\alpha_{10}(y, \eta, \tau_0) & = R_{11,11}(y, \eta, \tau_0) + R_{22,22}(y, \eta, \tau_0) - R_{11,22}(y, \eta, \tau_0) \\
& \quad - R_{22,11}(y, \eta, \tau_0) - 4R_{12,12}(y, \eta, \tau_0)
\end{aligned} \tag{33}$$

We note, here, under this condition, $R_{22,22} = R_{33,33}$; and $R_{12,12} = R_{13,13}$. At this stage we will find it helpful to rewrite $R_{ij,kl}$ explicitly in terms of the component terms: $R_{11,11}$, $R_{22,22}$, $R_{12,12}$ etc. If we substitute Eq. (33) into Eq. (32), the turbulent field tensor is

$$\begin{aligned}
R_{ij,kl}(y, \eta, \tau_0) = & [\delta_{ij}\delta_{kl} - \delta_{kl}\delta_{i1}\delta_{j1} - \delta_{ij}\delta_{k1}\delta_{l1} + \delta_{i1}\delta_{j1}\delta_{k1}\delta_{l1}]R_{22,22}(y, \eta, \tau_0) \\
& + [\delta_{ik}\delta_{jl} + \delta_{il}\delta_{jk} - 2\delta_{ij}\delta_{kl} + 2\delta_{kl}\delta_{i1}\delta_{j1} + 2\delta_{ij}\delta_{k1}\delta_{l1} \\
& - \delta_{jk}\delta_{i1}\delta_{l1} - \delta_{ik}\delta_{j1}\delta_{l1} - \delta_{il}\delta_{j1}\delta_{k1} - \delta_{jl}\delta_{i1}\delta_{k1}]R_{23,23}(y, \eta, \tau_0) \\
& + [\delta_{jk}\delta_{i1}\delta_{l1} + \delta_{ik}\delta_{j1}\delta_{l1} + \delta_{il}\delta_{j1}\delta_{k1} + \delta_{jl}\delta_{i1}\delta_{k1} - 4\delta_{i1}\delta_{j1}\delta_{k1}\delta_{l1}]R_{12,12}(y, \eta, \tau_0) \\
& + [\delta_{kl}\delta_{i1}\delta_{j1} - \delta_{i1}\delta_{j1}\delta_{k1}\delta_{l1}]R_{11,22}(y, \eta, \tau_0) \\
& + [\delta_{ij}\delta_{k1}\delta_{l1} - \delta_{i1}\delta_{j1}\delta_{k1}\delta_{l1}]R_{22,11}(y, \eta, \tau_0) \\
& + \delta_{i1}\delta_{j1}\delta_{k1}\delta_{l1}R_{11,11}(y, \eta, \tau_0)
\end{aligned} \tag{34}$$

Now, the Fourier transform of $R_{ij,kl}(y, \eta, \tau_0)$ is just a straightforward application of the integral definition given by Eq. (20), hence

$$\begin{aligned}
\hat{R}_{ij,kl}(y, \eta, \omega) = & [\delta_{ij}\delta_{kl} - \delta_{kl}\delta_{i1}\delta_{j1} - \delta_{ij}\delta_{k1}\delta_{l1} + \delta_{i1}\delta_{j1}\delta_{k1}\delta_{l1}]\hat{R}_{22,22}(y, \eta, \omega) \\
& + [\delta_{ik}\delta_{jl} + \delta_{il}\delta_{jk} - 2\delta_{ij}\delta_{kl} + 2\delta_{kl}\delta_{i1}\delta_{j1} + 2\delta_{ij}\delta_{k1}\delta_{l1} \\
& - \delta_{jk}\delta_{i1}\delta_{l1} - \delta_{ik}\delta_{j1}\delta_{l1} - \delta_{il}\delta_{j1}\delta_{k1} - \delta_{jl}\delta_{i1}\delta_{k1}]\hat{R}_{23,23}(y, \eta, \omega) \\
& + [\delta_{jk}\delta_{i1}\delta_{l1} + \delta_{ik}\delta_{j1}\delta_{l1} + \delta_{il}\delta_{j1}\delta_{k1} + \delta_{jl}\delta_{i1}\delta_{k1} - 4\delta_{i1}\delta_{j1}\delta_{k1}\delta_{l1}]\hat{R}_{12,12}(y, \eta, \omega) \\
& + [\delta_{kl}\delta_{i1}\delta_{j1} - \delta_{il}\delta_{j1}\delta_{k1}]\hat{R}_{11,22}(y, \eta, \omega) \\
& + [\delta_{ij}\delta_{k1}\delta_{l1} - \delta_{i1}\delta_{j1}\delta_{k1}]\hat{R}_{22,11}(y, \eta, \omega) \\
& + \delta_{i1}\delta_{j1}\delta_{k1}\delta_{l1}\hat{R}_{11,11}(y, \eta, \omega)
\end{aligned} \tag{35}$$

4.2. Power spectral density

The final step that remains is the power spectral density formula. Using Eq. (25) we get:

$$\begin{aligned}
\hat{P}(x, \omega) = & \int_{v_\infty(y)} [\hat{I}_{jjkk}(y, \omega | x) - \hat{I}_{11kk}(y, \omega | x) - \hat{I}_{kk11}(y, \omega | x) + \hat{I}_{1111}(y, \omega | x)]\hat{R}_{22,22}^{\text{total}}(y, \omega)d^3y \\
& + \int_{v_\infty(y)} [\hat{I}_{jjkj}(y, \omega | x) + \hat{I}_{jjjk}(y, \omega | x) - 2\hat{I}_{jjkk}(y, \omega | x) + 2\hat{I}_{11kk}(y, \omega | x) + 2\hat{I}_{kk11}(y, \omega | x) \\
& - \hat{I}_{1kk1}(y, \omega | x) - \hat{I}_{k1k1}(y, \omega | x) - \hat{I}_{k11k}(y, \omega | x) - \hat{I}_{1k1k}(y, \omega | x)]\hat{R}_{23,23}^{\text{total}}(y, \omega)d^3y \\
& + \int_{v_\infty(y)} [\hat{I}_{1kk1}(y, \omega | x) + \hat{I}_{k1k1}(y, \omega | x) + \hat{I}_{k11k}(y, \omega | x) + \hat{I}_{1k1k}(y, \omega | x) - 4\hat{I}_{1111}(y, \omega | x)]\hat{R}_{12,12}^{\text{total}}(y, \omega)d^3y \\
& + \int_{v_\infty(y)} [\hat{I}_{11kk}(y, \omega | x) - \hat{I}_{1111}(y, \omega | x)]\hat{R}_{11,22}^{\text{total}}(y, \omega)d^3y \\
& + \int_{v_\infty(y)} [\hat{I}_{kk11}(y, \omega | x) - \hat{I}_{1111}(y, \omega | x)]\hat{R}_{22,11}^{\text{total}}(y, \omega)d^3y \\
& + \int_{v_\infty(y)} [\hat{I}_{1111}(y, \omega | x)]\hat{R}_{11,11}^{\text{total}}(y, \omega)d^3y
\end{aligned} \tag{36}$$

4.4. Correlation functions in Eq. (34)

The correlation functions in Eq. (34) could, in principle, take any form. By calculating them using the LES data we found their behaviour was Gaussian-like, and the characteristic scales defining the Gaussian fit were similar to $R_{11,11}(y, \eta, \tau_0)$. In this paper, then, we suppose they are simply a constant multiple of $R_{11,11}(y, \eta, \tau_0)$, where $R_{11,11}(y, \eta, \tau_0)$ is given by Eq. (30).

$$\begin{aligned}
R_{22,22}(y, \eta, \tau_0) &= \mu R_{11,11}(y, \eta, \tau_0) \\
R_{12,12}(y, \eta, \tau_0) &= \nu R_{11,11}(y, \eta, \tau_0) \\
R_{23,23}(y, \eta, \tau_0) &= \zeta R_{11,11}(y, \eta, \tau_0) \\
R_{11,22}(y, \eta, \tau_0) &= \chi R_{11,11}(y, \eta, \tau_0)
\end{aligned} \tag{37}$$

(We have let $R_{11,22}(y, \eta, \tau_0) = R_{22,11}(y, \eta, \tau_0)$). Now the power spectral density equation takes a much simpler form,

$$\begin{aligned}
\hat{P}(x, \omega) = & \mu \int_{v_\infty(y)} [\hat{I}_{jjkk}(y, \omega | x) - \hat{I}_{11kk}(y, \omega | x) - \hat{I}_{kk11}(y, \omega | x) + \hat{I}_{1111}(y, \omega | x)] \hat{R}_{11,11}^{\text{total}}(y, \omega) d^3 y \\
+ & \zeta \int_{v_\infty(y)} [\hat{I}_{jjkj}(y, \omega | x) + \hat{I}_{jkjk}(y, \omega | x) - 2\hat{I}_{jjkk}(y, \omega | x) + 2\hat{I}_{11kk}(y, \omega | x) + 2\hat{I}_{kk11}(y, \omega | x) \\
& - \hat{I}_{1kk1}(y, \omega | x) - \hat{I}_{k1k1}(y, \omega | x) - \hat{I}_{k11k}(y, \omega | x) - \hat{I}_{1k1k}(y, \omega | x)] \hat{R}_{11,11}^{\text{total}}(y, \omega) d^3 y \\
& + \nu \int_{v_\infty(y)} [\hat{I}_{1kk1}(y, \omega | x) + \hat{I}_{k1k1}(y, \omega | x) + \hat{I}_{k11k}(y, \omega | x) + \hat{I}_{1k1k}(y, \omega | x) - 4\hat{I}_{1111}(y, \omega | x)] \hat{R}_{11,11}^{\text{total}}(y, \omega) d^3 y \\
+ & \chi \int_{v_\infty(y)} [\hat{I}_{11kk}(y, \omega | x) + \hat{I}_{kk11}(y, \omega | x) - 2\hat{I}_{1111}(y, \omega | x)] \hat{R}_{11,11}^{\text{total}}(y, \omega) d^3 y \\
& + \int_{v_\infty(y)} [\hat{I}_{1111}(y, \omega | x)] \hat{R}_{11,11}^{\text{total}}(y, \omega) d^3 y
\end{aligned} \tag{38}$$

4.5. Predicted noise spectra

We analyse Eq. (38) as before. The coefficients (μ, ζ, ν) are easily determined using the LES data at the location along the shear layer towards the end of the potential core ($y_1 = 4D_{\text{jet}}$ and $r = 0.5D_{\text{jet}}$). We compute the correlation functions we require (in Eq. 38), and find the ratio of their amplitudes to $R_{11,11}$. In Fig. (4a) we show the predicted noise spectrum at 90° , and in Fig. (4b) we show peak jet noise spectrum at 30° to the jet axis. The 30° spectrum is similar to the condition of isotropy, and the predictions are very good in comparison to experiment. However, the peak noise we predict at 90° is about 5 dB higher than experiment.

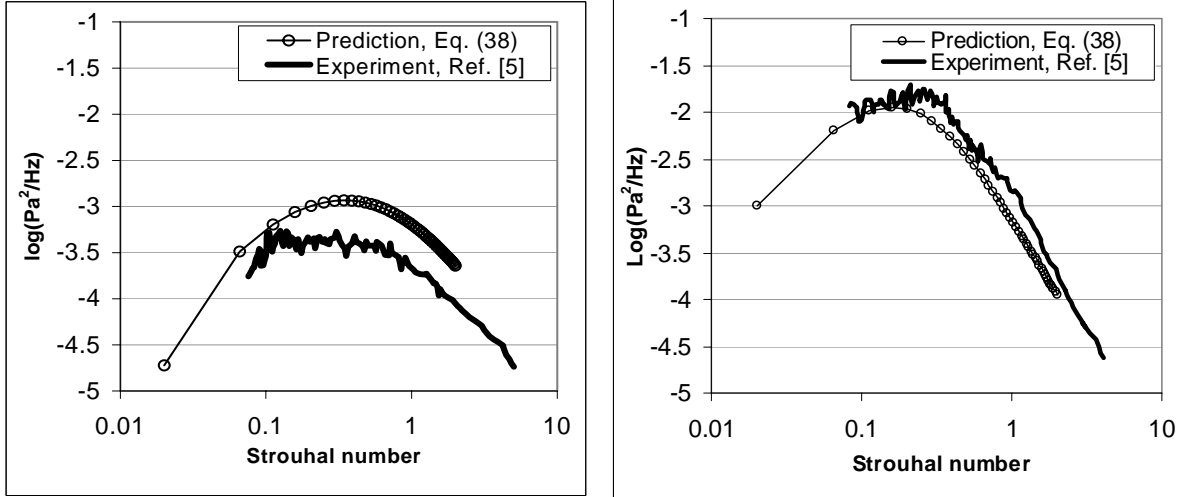


Figure 4: Condition of Statistical Anisotropic: comparison of predictions made using Eq. (38) and Experiment⁵. Strouhal Number = $\omega D_{jet} / 2\pi U_{jet}$ (ω is the angular frequency rad/s; D_{jet} is the nozzle exit diameter, and U_{jet} is the nozzle exit velocity).

5. APPROXIMATION OF STATISTICAL ANISOTROPY

So far we have proceeded formally; Eq. (36) was just an exact representation of $R_{ij,kl}$ with the condition of axial symmetry. But, as it stands Eq. (36) is computationally demanding; it requires 6 correlation functions which all depend upon a well resolved LES solution. Small inaccuracies in that solution, may be amplified by the simplification introduced in the propagation model. We based the wave propagation on a locally parallel mean flow; this, however, ignores jet evolution effects. Moreover, we neglected the variation of the second rank wave propagation tensor in the jet cross plane—see Eq (21). That approximation can introduce error as well, because, the radial derivative of the axial Green function involves a radial derivative of the mean velocity, which varies rapidly across the shear layer¹². Taken together, these approximations may affect the power spectral density significantly because of the cancellations within the integrand.

For example, consider the deviatoric term $R_{23,23}$ which represents out of plane shear. The LES data showed the amplitude of $R_{23,23}$ was relatively small in comparison to $R_{11,11}$, $R_{22,22}$ and $R_{12,12}$. However, $R_{23,23}$ may be subject to a high ‘signal-to-noise ratio’ since it requires high accuracy in both cross-plane directions, 2, and 3. Preserving numerical accuracy is especially challenging closer to the nozzle, where the shear layer gradients are finer, however, this region is important because it makes a significant contribution to the overall sound power at large angles to the jet axis¹³. So the final step we take is an approximation of the formal condition of anisotropy, designed to retain only three components: $R_{11,11}$, $R_{22,22}$ and $R_{12,12}$.

5.1. Definition

We start with Eq. (32); $R_{ij,kl}(y, \eta, \tau_0)$ is re-written supposing it is symmetric about the axial direction, and where the symmetries between the tensor indices have been applied.

$$\begin{aligned}
R_{ij,kl}(y, \eta, \tau_0) = & \delta_{ij}\delta_{kl}\alpha_1(y, \eta, \tau_0) + [\delta_{ik}\delta_{jl} + \delta_{il}\delta_{jk}] \alpha_2(y, \eta, \tau_0) \\
& + \delta_{kl}\delta_{il}\delta_{j1}\alpha_4(y, \eta, \tau_0) + \delta_{ij}\delta_{k1}\delta_{l1}\alpha_5(y, \eta, \tau_0) \\
& + [\delta_{jl}\delta_{i1}\delta_{k1} + \delta_{ik}\delta_{j1}\delta_{l1} + \delta_{jk}\delta_{i1}\delta_{l1} + \delta_{il}\delta_{j1}\delta_{k1}] \alpha_6(y, \eta, \tau_0) \\
& + \delta_{i1}\delta_{j1}\delta_{k1}\delta_{l1}\alpha_{10}(y, \eta, \tau_0)
\end{aligned} \tag{39}$$

Now we simplify this equation by approximation. Suppose:

$$\begin{aligned}
\alpha_1(y, \eta, \tau_0) &= \alpha_2(y, \eta, \tau_0) \\
\alpha_4(y, \eta, \tau_0) &= \alpha_5(y, \eta, \tau_0) = \alpha_6(y, \eta, \tau_0)
\end{aligned} \tag{40}$$

This approximation is pragmatic. Since we know, the correlation functions are difficult to resolve numerically, and in particular $R_{23,23}$. We apply the approximation at the stage of Eq. (32)—where the turbulent field tensor is expressed in terms of the scalar functions, $\alpha_{1\dots 10}(y, \eta, \tau_0)$ —so that the power spectral density is as simple as possible. Hence,

$$\begin{aligned}
R_{ij,kl}(y, \eta, \tau_0) \approx & [\delta_{ij}\delta_{kl} + \delta_{ik}\delta_{jl} + \delta_{il}\delta_{jk}] \alpha_2(y, \eta, \tau_0) \\
& + [\delta_{jl}\delta_{i1}\delta_{k1} + \delta_{ik}\delta_{j1}\delta_{l1} + \delta_{jk}\delta_{i1}\delta_{l1} + \delta_{il}\delta_{j1}\delta_{k1} + \delta_{kl}\delta_{i1}\delta_{j1} + \delta_{ij}\delta_{k1}\delta_{l1}] \alpha_6(y, \eta, \tau_0) \\
& + \delta_{i1}\delta_{j1}\delta_{k1}\delta_{l1}\alpha_{10}(y, \eta, \tau_0)
\end{aligned} \tag{41}$$

The scalar functions are found in the usual way. For brevity we omit those steps and proceed directly to the Fourier transform of Eq. (41),

$$\begin{aligned}
\hat{R}_{ij,kl}(y, \eta, \omega) = & [\delta_{ij}\delta_{kl} + \delta_{ik}\delta_{jl} + \delta_{il}\delta_{jk} - \delta_{jl}\delta_{i1}\delta_{k1} - \delta_{jk}\delta_{i1}\delta_{l1} - \delta_{il}\delta_{j1}\delta_{k1} \\
& - \delta_{ik}\delta_{j1}\delta_{l1} - \delta_{ik}\delta_{j1}\delta_{l1} - \delta_{ij}\delta_{k1}\delta_{l1} - \delta_{kl}\delta_{i1}\delta_{j1} + \delta_{il}\delta_{j1}\delta_{k1}\delta_{l1}] \frac{\hat{R}_{22,22}}{3}(y, \eta, \omega) \\
& + [\delta_{jk}\delta_{i1}\delta_{l1} + \delta_{ik}\delta_{j1}\delta_{l1} + \delta_{il}\delta_{j1}\delta_{k1} + \delta_{jl}\delta_{i1}\delta_{k1} + \delta_{ij}\delta_{k1}\delta_{l1} + \delta_{il}\delta_{j1}\delta_{kl} - 6\delta_{i1}\delta_{j1}\delta_{k1}\delta_{l1}] \hat{R}_{12,12}(y, \eta, \omega) \\
& + \delta_{i1}\delta_{j1}\delta_{k1}\delta_{l1} \hat{R}_{11,11}(y, \eta, \omega)
\end{aligned} \tag{42}$$

5.2. Power spectral density

The power spectral density formula is found using Eq. (25),

$$\begin{aligned}
\hat{P}(x, \omega) = & \int_{v_\infty(y)} [\hat{I}_{jjkk}(y, \omega | x) + \hat{I}_{jjkj}(y, \omega | x) + \hat{I}_{jjjk}(y, \omega | x) - \hat{I}_{k1k1}(y, \omega | x) - \hat{I}_{k11k}(y, \omega | x) \\
& - \hat{I}_{1kk1}(y, \omega | x) - \hat{I}_{1k1k}(y, \omega | x) - \hat{I}_{kk11}(y, \omega | x) - \hat{I}_{11kk}(y, \omega | x) + 3\hat{I}_{1111}(y, \omega | x)] \frac{\hat{R}_{22,22}^{\text{total}}(y, \omega) d^3 y}{3} \\
& + \int_{v_\infty(y)} [\hat{I}_{k1k1}(y, \omega | x) + \hat{I}_{k11k}(y, \omega | x) + \hat{I}_{1kk1}(y, \omega | x) + \hat{I}_{1k1k}(y, \omega | x) \\
& + \hat{I}_{kk11}(y, \omega | x) + \hat{I}_{11kk}(y, \omega | x) - 6\hat{I}_{1111}(y, \omega | x)] \hat{R}_{12,12}^{\text{total}}(y, \omega) d^3 y \\
& + \int_{v_\infty(y)} [\hat{I}_{1111}(y, \omega | x)] \hat{R}_{11,11}^{\text{total}}(y, \omega) d^3 y
\end{aligned}$$

(43)

5.3. Correlation functions: $R_{22,22}(y, \eta, \tau_0)$ and $R_{12,12}(y, \eta, \tau_0)$

As we have done throughout this paper we suppose the correlation functions $R_{22,22}$ and $R_{12,12}$ are simply a constant multiple of $R_{11,11}(y, \eta, \tau_0)$. Viz.:

$$R_{22,22}(y, \eta, \tau_0) = \mu R_{11,11}(y, \eta, \tau_0) \text{ and } R_{12,12}(y, \eta, \tau_0) = \nu R_{11,11}(y, \eta, \tau_0).$$

Then the power spectral density equation becomes:

$$\begin{aligned}
\hat{P}(x, \omega) = & \mu \int_{v_\infty(y)} [\hat{I}_{jjkk}(y, \omega | x) + \hat{I}_{jjkj}(y, \omega | x) + \hat{I}_{jjjk}(y, \omega | x) - \hat{I}_{k1k1}(y, \omega | x) - \hat{I}_{k11k}(y, \omega | x) \\
& - \hat{I}_{1kk1}(y, \omega | x) - \hat{I}_{1k1k}(y, \omega | x) - \hat{I}_{kk11}(y, \omega | x) - \hat{I}_{11kk}(y, \omega | x) + 3\hat{I}_{1111}(y, \omega | x)] \frac{\hat{R}_{11,11}^{\text{total}}(y, \omega) d^3 y}{3} \\
& + \nu \int_{v_\infty(y)} [\hat{I}_{k1k1}(y, \omega | x) + \hat{I}_{k11k}(y, \omega | x) + \hat{I}_{1kk1}(y, \omega | x) + \hat{I}_{1k1k}(y, \omega | x) \\
& + \hat{I}_{kk11}(y, \omega | x) + \hat{I}_{11kk}(y, \omega | x) - 6\hat{I}_{1111}(y, \omega | x)] \hat{R}_{11,11}^{\text{total}}(y, \omega) d^3 y \\
& + \int_{v_\infty(y)} [\hat{I}_{1111}(y, \omega | x)] \hat{R}_{11,11}^{\text{total}}(y, \omega) d^3 y.
\end{aligned}$$

(44)

5.4. Predicted noise spectra

In Fig. (5a) we show the predicted noise spectrum at 90° , and in Fig. (5b) we show peak jet noise spectrum at 30° to the jet axis. Although the 30° spectrum is similar to formal condition of anisotropy (and to experiment), the 90° predictions now are very good and within 1 dB of experiment.

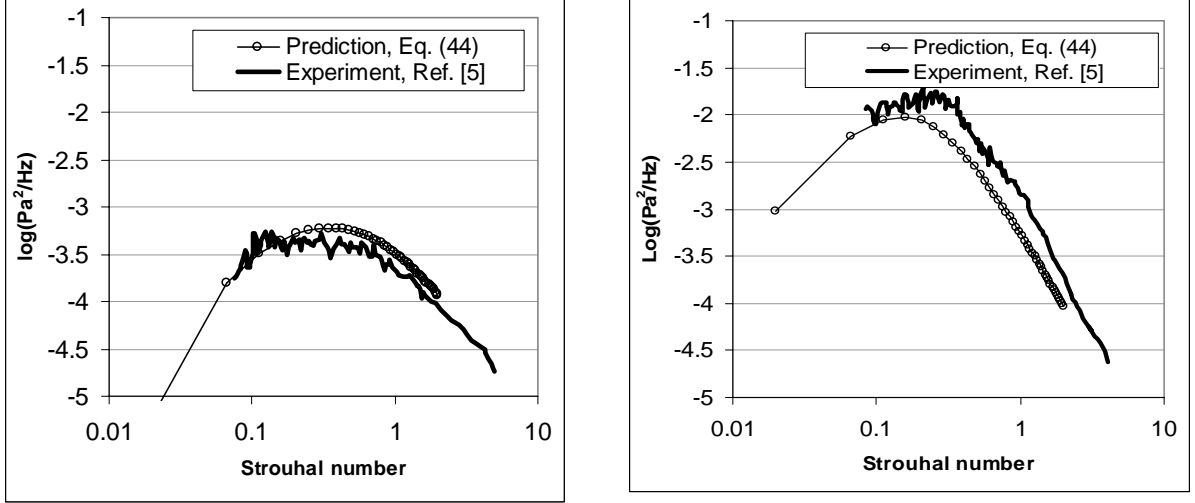


Figure 5: Anisotropic Approximation: comparison of predictions made using Eq. (44) and Experiment⁵. Strouhal Number = $\omega D_{jet} / 2\pi U_{jet}$ (ω is the angular frequency rad/s; D_{jet} is the nozzle exit diameter, and U_{jet} is the nozzle exit velocity).

6. CONCLUSION

In this paper, we have formulated a hierarchy of jet noise models by examining the kinematic representation for the cross power spectral density of the Reynolds stress source term. The hierarchy began with the condition of isotropy and we went on to develop a series anisotropic models. We have shown anisotropy does not affect the noise spectrum at small observation angles, like 30° . This is because, at very small observation angles, a low frequency term dominates the jet noise spectrum, and accounts entirely for the peak noise¹². The low frequency term exists even under the condition of isotropy¹⁴. However, anisotropy does affect the sound predictions at higher angles, 90° for example, as Goldstein and Rosenbaum found⁴. At higher observation angles, this effect of anisotropy is more important on the prediction than the effect jet evolution on the wave propagation terms. But, having said that, a complete form of anisotropy may deliver a power spectral density formula that is susceptible to numerical errors and should be used with caution. By approximating the formal condition of anisotropy, to avoid correlation functions that may be difficult to resolve accurately, we obtained a simpler formula for the power spectrum. The approximate anisotropic model gives very good jet noise predictions across the spectrum. Both at 30° and 90° the predictions are within 3 dB of the data from experiment.

Acknowledgments

This work is part of a collaborative project on jet noise funded by the Engineering and Physical Sciences Research Council (EPSRC) whose support is gratefully acknowledged. SAK acknowledges, with gratitude, the support of the Royal Society of London. We are all grateful for helpful discussions with colleagues at the University of Loughborough and Rolls-Royce, particularly Professor Jim McGuirk, Drs Gary Page and Jason Wu who made his LES solution readily available to us.

6. REFERENCES

- [1]. Lighthill, M.J., "On sound generated aerodynamically: I. General theory," Proceedings of the Royal Society of London A, vol. 222, 1952, pp. 564-587.
- [2]. Kraichnan, R.H., "The pressure field within homogeneous anisotropic turbulence," Journal of the Acoustical Society of America, vol. 28, No. 1, 1956, pp. 64-72.
- [3]. Goldstein, M.E., and Rosenbaum, B., "The effect of anisotropic turbulence on aerodynamic noise," Journal of the Acoustical Society of America, vol. 54, No. 3, 1973, pp. 630-645.
- [4]. Goldstein, M.E., "A unified approach to some recent developments in jet noise theory," Journal of Aeroacoustics, vol. 1, No. 1, 2002, pp. 1-16.
- [5]. Jordan, P., and Gervais, P., "Modelling self- and shear-noise mechanisms in inhomogeneous, anisotropic turbulence, Journ. Sound and Vibration", 279 (2005), pp. 529-555
- [6]. Dowling, A.P., Ffowcs Williams, J.E and Goldstein, M.E., "Sound production in a moving stream," Proceedings of the Royal Society of London A, vol. 288, 1978, pp. 321-349.
- [7]. Tam, C.K.W., and Auriant, L., "Mean flow refraction effects on sound radiated from localized sources in a jet," Journal of Fluid Mechanics, vol. 370, 1998, pp. 149-174.
- [8]. Crighton et al., Modern methods in analytical acoustics, Springer-Verlag, 1994, pp. 80-116.
- [9]. Tam, C.K.W., and Auriant, L., "Jet mixing noise from fine scale turbulence," AIAA Journal, vol. 206, No. 2, 1999, pp. 145-153.
- [10]. Afsar, M.Z., Dowling, A.P., and Karabasov, S.A., "Comparison of jet noise models," 12th AIAA-CEAS Aeroacoustics Conference, Boston, USA, May 2006.
- [11]. Wu, X., McGuirk, J.J., Tristante, I.H. and Page, G.J., "Influence of Nozzle Modelling in LES of Turbulent Free Jets", AIAA-2005-2883, 11th AIAA/CEAS Aeroacoustics Conference, Monterey, California, USA, May 2005, pp 1-8.
- [12]. Karabasov, S.A., Hynes, T.P., and Dowling, A.P. "Effect of mean-flow evolution on sound propagation through non-uniform jet flows", AIAA-2007-3655, 13-th AIAA/CEAS conference, Rome, Italy, 2007.
- [13] Bogey, C., Bailly, C. and Juve, D. 2003 "Noise investigation of a high subsonic, moderate Reynolds number jet using a compressible LES". Theoret. Comput. Fluid Dynamics 16(4), pp. 273-297.
- [14]. Afsar, M.Z., Dowling, A.P., and Karabasov, S.A., "Jet noise in the zone of silence," 13th AIAA-CEAS Aeroacoustics Conference.